



Chymase released from hypoxia-activated cardiac mast cells cleaves human apoA-I at Tyr¹⁹² and compromises its cardioprotective activity^S

Ilona Kareinen,^{*,†} Marc Baumann,[§] Su Duy Nguyen,^{*} Katariina Maaninka,^{*} Andrey Anisimov,^{***} Minoru Tozuka,^{††} Matti Jauhiainen,^{§§} Miriam Lee-Rueckert,^{*} and Petri T. Kovanen^{1,*}

Wihuri Research Institute,^{*} Helsinki, Finland; Department of Veterinary Biosciences, Faculty of Veterinary Medicine,[†] Protein Chemistry Unit, Institute of Biomedicine/Anatomy,[§] and Translational Cancer Biology Program,^{**} University of Helsinki, Helsinki, Finland; Analytical Laboratory Chemistry,^{††} Graduate School of Health Care Sciences, Tokyo Medical and Dental University, Tokyo, Japan; Minerva Foundation Institute for Medical Research,^{§§} Helsinki, Finland; and National Institute for Health and Welfare,^{***} Helsinki, Finland

Abstract ApoA-I, the main structural and functional protein of HDL particles, is cardioprotective, but also highly sensitive to proteolytic cleavage. Here, we investigated the effect of cardiac mast cell activation and ensuing chymase secretion on apoA-I degradation using isolated rat hearts in the Langendorff perfusion system. Cardiac mast cells were activated by injection of compound 48/80 into the coronary circulation or by low-flow myocardial ischemia, after which lipid-free apoA-I was injected and collected in the coronary effluent for cleavage analysis. Mast cell activation by 48/80 resulted in apoA-I cleavage at sites Tyr¹⁹² and Phe²²⁹, but hypoxic activation at Tyr¹⁹² only. In vitro, the proteolytic end-product of apoA-I with either rat or human chymase was the Tyr¹⁹²-truncated fragment. This fragment, when compared with intact apoA-I, showed reduced ability to promote migration of cultured human coronary artery endothelial cells in a wound-healing assay. We propose that C-terminal truncation of apoA-I by chymase released from cardiac mast cells during ischemia impairs the ability of apoA-I to heal damaged endothelium in the ischemic myocardium.—Kareinen, I., M. Baumann, S. D. Nguyen, K. Maaninka, A. Anisimov, M. Tozuka, M. Jauhiainen, M. Lee-Rueckert, and P. T. Kovanen. Chymase released from hypoxia-activated cardiac mast cells cleaves human apoA-I at Tyr¹⁹² and compromises its cardioprotective activity. *J. Lipid Res.* 2018. 59: 945–957.

Supplementary key words apolipoproteins • carboxyl-terminal truncation • cardiac ischemia • cells and tissues/endothelial cells • diseases/atherosclerosis • high density lipoproteins • reconstituted high density lipoprotein • mass spectrometry • proteolysis

ApoA-I, the main protein component of HDLs, is a 243 amino acid polypeptide with an apparent molecular mass of ~28,000 Da. Circulating HDL particles contain either a single copy or multiple copies of apoA-I (1). Besides its role in HDL structure, apoA-I is also critical for HDL functionality (2). ApoA-I, both in lipid-free form and in the nascent lipid-poor form (pre β ₁-HDL), promotes efflux of cholesterol via the ABCA1 transporter from macrophage foam cells and so initiates the reverse cholesterol transport pathway from these cells, which is followed by facilitated hepatic uptake and ultimately excretion of the macrophage-derived cholesterol by the gut (2–4). Importantly, lipid-poor apoA-I particles are abundant in interstitial fluids, where they can accept excess cholesterol from cholesterol-loaded cells (5). Recent data suggest that, by regulating cellular cholesterol homeostasis, HDL and apoA-I can also regulate inflammatory responses in endothelial cells and other types of cells that have been activated by proinflammatory stimuli in the arterial intima (6). Moreover, apoA-I has a major role in binding the endotoxin (lipopolysaccharide; LPS) released from the surface membrane of Gram-negative bacteria and thereby neutralizes its toxic effects on endothelial cells (7).

Mast cells are proinflammatory cells, which, upon activation and ensuing degranulation, release a variety of granule-bound neutral proteases, notably chymase, into the surrounding extracellular fluid (8). In the extracellular fluid, the soluble components of the granules, such as histamine and soluble proteoglycans, disperse, whereas most

The Wihuri Research Institute is maintained by Jenny ja Antti Wihurin Rahasto (Jenny and Antti Wihuri Foundation). This study was partially supported by Suomen Eläinlääketieteen Säätiö (Finnish Foundation of Veterinary Research) (I.K.), Veritas Foundation (I.K. and M.L.-R.), Aarne Koskelon Säätiö (Aarne Koskelo Foundation) (M.L.-R.), and the Research Council for Health, Academy of Finland (M.J.).

Manuscript received 2 May 2017 and in revised form 22 March 2018.

Published, *JLR Papers in Press*, March 26, 2018

DOI <https://doi.org/10.1194/jlr.M077503>

Abbreviations: 48/80, compound 48/80; BTEE, Nbenzoyl-L-tyrosine ethyl ester; HCAEC, human coronary artery endothelial cell; IRI, ischemia/reperfusion injury; LPS, lipopolysaccharide; rHDL, reconstituted HDL; SBTI, soybean trypsin inhibitor.

¹To whom correspondence should be addressed.

email: petri.kovanen@wri.fi

^S The online version of this article (available at <http://www.jlr.org>) contains a supplement.

of chymase remains attached to the insoluble proteoglycan fraction of the granules forming functional composite superstructures, which we have designated granule remnants (9). Mast cells in the rat heart express chymase, which, like its human counterpart, is a chymotryptic enzyme (8, 10, 11). Of note, studies on degranulated rat mast cells have shown that the binding of chymase to the heparin proteoglycans in the exocytosed granule remnants confers chymase partial resistance to its natural inhibitors present in the extracellular fluids, such as the arterial intimal fluid (12). As a serine protease with chymotrypsin-like primary substrate specificity, chymase cleaves peptide bonds preferentially after aromatic amino acids with the order of preference Phe>Tyr>Trp (8). Importantly, chymase of either rodent or human origin efficiently cleaves lipid-free and lipid-poor forms of apoA-I *in vitro*, so compromising the ABCA1-mediated cholesterol efflux pathway, and studies *in vivo* indicate that such proteolysis can also occur in specific tissue fluids in which these preferred apolipoprotein substrates are abundantly present (9). Indeed, systemic activation of mast cells with ensuing degranulation during anaphylactic shock in the mouse proteolytically modifies circulating HDL and reduces the capacity of anaphylactic serum to act as cholesterol acceptor from cultured macrophage foam cells (13).

The initial indication for a role of chymase in myocardial pathology derives from the observation that chymase is the major angiotensin II-forming enzyme in the human heart (10). Cardiac chymase has also been shown to induce adverse cardiac remodeling after estrogen depletion in experimental rat models (11, 14). Moreover, other reports demonstrate that cardiac chymase contributes to the development of the adverse effects of hypertensive heart failure in rats (15) and that it promotes acute ischemia/reperfusion injury (IRI) in pigs (16). Importantly, in the experimental pig model, inhibition of cardiac mast cell-derived chymase resulted in decreased infarction size after IRI, thus making chymase alone responsible for at least some of the harmful effects of IRI (16). Similarly, complete degranulation of cardiac mast cells shortly before IRI in rats has been shown to attenuate inflammation and to result in improved cardiac function due to a decrease in the release of cytotoxic mediators from such granule-deficient cardiac mast cells during IRI (17).

Both human plasma HDL and reconstituted HDL (rHDL) have been found to exert cardioprotective effects in experimental IRI in rats (18, 19). Thus, it was shown that administration of HDL before ischemia in an isolated rat heart model reduces cardiac TNF- α content and increases prostaglandin release, resulting in improved postischemic functional recovery. Importantly, this effect was attenuated when either type of HDL was administered during the reperfusion phase, revealing that in order to exhibit cardioprotective properties, HDL has to be infused before but not during reperfusion to prevent attenuation of their functionality. Such partial loss of the ability of HDL to preserve myocardial function when injected into the coronary circulation in the postischemic phase was explained by an emerging resistance of the myocardium to the cardioprotective effects

of HDL (18, 19). Another explanation is that the loss of cardioprotection may actually have resulted from HDL becoming dysfunctional already during cardiac ischemia, i.e., during the time period preceding the onset of reperfusion. Since IRI in hearts isolated from rats (17, 20), dogs (21), guinea pigs, and mice (22) induces cardiac mast cell activation with ensuing chymase release, these findings actually suggest a pathological scenario in which chymase could promote local proteolysis of apoA-I.

Given that mast cell chymase can degrade apoA-I in interstitial fluids, e.g., in aortic intimal fluid (23), here, we studied the ability of chymase exocytosed by hypoxia-activated rat cardiac mast cells to proteolyze apoA-I when it is infused into the coronary circulation using the Langendorff isolated heart perfusion system. The results demonstrate that cardiac mast cell activation in the ischemic isolated rat heart is associated with the production of a C-terminally truncated apoA-I fragment, which we could identify as a proteolytic product generated solely by mast cell chymase. Of note, such proteolytic cleavage reduced the ability of apoA-I to promote migration of cultured human endothelial cells, when assessed using a wound healing assay. The results suggest that activated mast cells in the ischemic heart may compromise the ability of apoA-I to maintain endothelial integrity in the microvascular coronary arterial tree.

MATERIALS AND METHODS

Materials

Heparin Leo Orifarm (5,000 IU/ml) and isoflurane were purchased from Orion Pharmaceuticals (Espoo, Finland). Purified human lipid-free apoA-I has been kindly provided by Dr. Peter Lerch (Swiss Red Cross, Bern, Switzerland). Poorly lipidated apoA-I-containing rHDL were prepared by the cholate dialysis method as previously described (24) and used within a week. The final rHDL preparation (human apoA-I:egg yolk phosphatidyl choline:cholesterol, 1:30:12.5, mol/mol/mol ratio) exhibited pre β -mobility in agarose gel electrophoresis. The polyclonal anti-human apoA-I antibody R261 was produced in New Zealand white rabbits using purified lipid-free apoA-I as antigen. Compound 48/80 (48/80), phthaldialdehyde (OPTA), histamine dihydrochloride, *N*-benzoyl-L-tyrosine ethyl ester (BTEE), and soybean trypsin inhibitor (SBTI) were purchased from Sigma Aldrich. Recombinant human chymase (specific activity 80 BTEE units/ μ g) expressed in the baculovirus-insect cell system was kindly provided by Dr. Hidenori Kasai (Teijin Ltd. Co., Shizuoka, Japan). The preparation was diluted in a buffer containing 5 mM Tris-HCl, 150 mM NaCl, and 1 mM EDTA, pH 7.4 (TNE buffer) before use. The enzyme preparation was fully inhibited by adding SBTI at a final concentration of 100 μ g/ml. The mouse monoclonal antibody 16-4 Mab was used to detect the C-terminally truncated human apoA-I at the cleavage site Phe²²⁵, as previously described (25). Goat anti-rabbit Ig antibody P0448 and goat anti-mouse Ig antibody P0447 were purchased from Dako. Pierce ECL Western Blotting Substrate was from Thermo Scientific.

Animals

Experiments were conducted in conformity with the Finnish regulations and the Directive 2010/63/EU of the European Parliament on the protection of animals used for scientific purposes.

Animal experiments and the protocols were approved by The National Animal Experiment Board of Finland (ELLA; license no. ESAVI-2010-05448/Ym-23). Experiments were performed using female Wistar rats (200–250 g) purchased from Harlan Laboratories (Venray, The Netherlands). Rats were housed (three per cage), allowed to access regular rodent diet (Teklad Global, Harlan Laboratories) and water ad libitum, and maintained in an automatic 12/12 h dark–light cycle. Rats were kept in the animal facility at least for 1 week before experimentation.

Preparation of mast cell granule remnants

Rat peritoneal mast cells were obtained from euthanized rats by peritoneal lavage with PBS medium containing 0.5 mg/ml BSA, 1 mg/ml glucose, and 0.05 mg/ml heparin. Peritoneal cells present in the recovered PBS medium were sedimented by centrifugation at 200 *g* for 10 min, then resuspended in RPMI-medium, and cultured at 37°C in humidified CO₂ for 2 h to allow attachment of the peritoneal macrophages. After incubation, the medium was collected and centrifuged at 200 *g* for 5 min to sediment the nonadherent cells (mast cells). To obtain a maximum yield of the cytoplasmic secretory mast cell granules, the sedimented mast cells were resuspended in 0.3 M sucrose and lysed by subjecting them to 6 freeze-thaw cycles. Nonlysed mast cells and cellular debris were removed by centrifugation at 300 *g*, and the supernatant containing membrane-covered mast cell granules was collected. The supernatant was then centrifuged at 20,000 *g* for 30 min to sediment the granules, after which the granules were resuspended in distilled water to deprive them of membranes and thereby to convert them into “granule remnants” in which the heparin-bound chymase is exposed to the surrounding fluid. Finally, the granule remnants were resedimented to obtain a preparation of washed granule remnants. Chymase activity in mast cell granules was measured as described previously (26). In this assay, the BTEE units are calculated as $\Delta\text{abs}/\Delta\text{time} \times 1,000$ in 1 μl of mast cell lysate, and 1 BTEE unit corresponds to a 0.001 increase in absorbance per minute, when measured at 256 nm.

Incubation of apoA-I with human chymase and rat chymase

ApoA-I (1 mg/ml) was incubated at 37°C for the indicated periods of time in TNE buffer containing 40 BTEE units/ml either recombinant human chymase or rat chymase (present in granule remnants; see above). To stop proteolysis, each incubation vial was placed on ice. To inhibit the activity of recombinant human chymase, SBTI was added to the respective incubation vials. To remove rat granule remnant-bound chymase from the incubation mixtures, the vials were centrifuged at 10,000 *g* for 5 min at +4°C to remove the granule remnants. The apoA-I-containing supernatants were collected for later analysis or used in the wound-healing assay. All samples were stored at –80°C until analysis.

Isolation and perfusion of rat hearts in the Langendorff perfusion system

The *ex vivo* experiments were performed using the isolated heart perfusion according to Langendorff. For this purpose, rats were anesthetized using inhalation anesthesia (Univentor U-400, AgnTho's, Lidingö, Sweden) in a chamber saturated with 4% isoflurane, and anesthesia was maintained with 2.5% isoflurane with a rostral mask. Rats received *i.v.* injection of heparin (5,000 IU/kg) into the lateral tail vein. Anesthesia was then deepened by adjusting the vaporizer to 4% isoflurane, and once the pedal reflex was nonresponsive, ~4 ml of blood was collected from the vena cava caudalis in the terminally anesthetized animals. Hearts were then rapidly excised, mounted on the Langendorff apparatus, cannulated over the aortic valve, and perfused with Krebs-Henseleit

buffer (125 mM NaCl, 4.7 mM KCl, 20 mM NaHCO₃, 0.43 mM NaH₂PO₄, 1.0 mM MgCl₂, 1.3 mM CaCl₂, and 9.1 mM D-glucose; pH 7.4). The perfusion buffer was continuously purged with carbogen (95% O₂/5% CO₂) and maintained at 37°C. Hearts were equilibrated for 30 min at a flow rate of 6.6 ml/min before the mast cell activation-inducing treatments.

Degradation of apoA-I by activated cardiac mast cells in the Langendorff perfusion system

To study the effect of mast cell activation on the intactness of apoA-I perfused through the isolated rat heart, 1 mg of apoA-I in 100 μl of buffer was administered into the perfusion line near the inlet to the heart at a slow flow of 0.6 ml/min under the following conditions: after the 30 min equilibration period, immediately after a bolus injection of the mast cell degranulating 48/80 (300 μg in 500 μl of buffer) (Fig. 1A), or after low-flow ischemia induced by reducing the flow of the perfusion buffer to 0.6 ml/min for 20 min (Fig. 1B). Every compound was administered as a bolus injection into the perfusion line within a period of 1 min (for clarity, these short time intervals were not included in the time line shown in Fig. 1). After each apoA-I injection, fractions of the coronary effluent were collected at 0.6 ml/min flow for 5 min (1 fraction per min). When apoA-I was perfused into the system, a single protein peak eluted within 5 min after the injection. The fractions corresponding to the highest protein concentrations were taken for analysis of apoA-I proteolysis. In other experiments, 1 mg of apoA-I-containing rHDL (see Materials) was perfused through the rat hearts in the Langendorff system using the above described flow settings, and the intactness of apoA-I was evaluated in the fractions collected within 5 min after the injection, which contained the highest protein concentrations.

Morphological analysis of myocardial mast cells

Hearts were sectioned transversely and submerged into tissue section medium Tissue-Tek O.C.T. (Sakura Finetek Europe). Hearts were then rapidly frozen in liquid nitrogen and stored at –80°C until sectioned into 5 μm slices. The frozen sections were stained in 0.1% Toluidine blue, and the number of mast cells and the extent of mast cell activation were determined (magnification $\times 40$). Mast cell activation was defined as the presence of several extracellular granules extruded into the immediate vicinity of the parent cell and was determined as described previously (27).

Histamine determination

To establish the degree of myocardial mast cell activation, histamine was determined in all effluent samples collected during the Langendorff experimental protocols, as shown in Fig. 1. In short, the samples were precipitated with 50% TCA and centrifuged, and the precipitate was dissolved in 1 N NaOH and incubated with OPTA, which was used as the fluorescent reagent (28). After addition of 2 N H₂SO₄, the absorbance was measured in a spectrophotometer at excitation/emission 355/450 nm. Commercial histamine dihydrochloride was used as standard.

SDS-PAGE and Western blotting

ApoA-I proteolysis was evaluated by analyzing the collected effluent samples (1 μg protein) on NuPAGE Novex 4–12% Bis-Tris gradient gels (Life Technologies) under reducing conditions. The gels were stained with Instant Blue stain (Expediton), and the protein bands were documented by scanning the gels. For Western blotting analysis, the samples were first run on 15% SDS-PAGE under reducing conditions. Proteins were electrotransferred onto nitrocellulose membrane (Hybond-C Extra, Amersham). After blocking in 5% defatted milk, the membranes were incubated overnight at 4°C with either rabbit anti-human apoA-I polyclonal

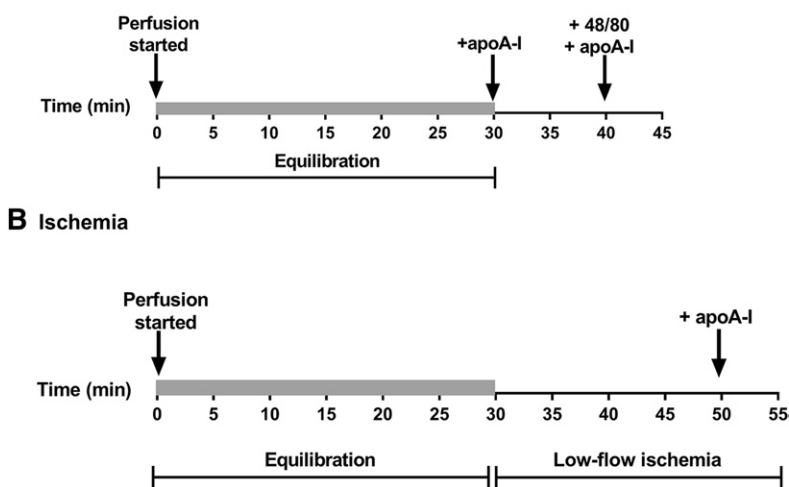


Fig. 1. Diagrammatic representation of cardiac mast cell activating protocols. Freshly isolated hearts were mounted in the Langendorff system, perfused with buffer at a flow rate of 6.6 ml/min during 30 min (“Equilibration,” denoted by the shaded areas), and then exposed to treatments inducing mast cell activation. A: ApoA-I (1 mg) was administered into the perfusion line at the flow rate of 0.6 ml/min immediately after equilibration (to act as a control) and again immediately after administration of 48/80. Fractions of the coronary effluent were collected for 5 min at the flow rate of 0.6 ml/min after each apoA-I injection, and the hearts were perfused with buffer before the second dose of apoA-I. B: ApoA-I (1 mg) was administered into the perfusion line after a 20 min period of low-flow ischemia at the flow rate of 0.6 ml/min, and effluent samples were collected for 5 min.

antibody (R261, diluted 1:2,000) or mouse anti-human C-terminally truncated apoA-I monoclonal antibody (164 Mab, diluted 1:1,000). The membranes were then incubated at room temperature for 1 h with either goat-anti-rabbit IgG antibody (diluted 1:2,000) or with goat-anti-mouse IgM antibody (diluted 1:5,000). Immune complexes were visualized with HRP-conjugated ECL. Ponceau S staining was used to confirm even protein transfer to nitrocellulose and equivalent protein mass loading.

MALDI-TOF MS

The degradation products of apoA-I generated either in the Langendorff perfusion system (coronary effluent) or by incubating apoA-I with human or rat chymase *in vitro* (total incubation mixture) were identified by MALDI-TOF MS. MALDI-TOF and TOF/TOF analyses were carried out with an UltraFleXtreme 2000 Hz laser instrument (Bruker Daltonics, Bremen, Germany) equipped with a SmartBeam™ Nd/YAG laser (355 nm), operated in positive and linear modes. Typically, a mass spectrum was acquired by accumulating spectra of 2,000 and up to 20,000 laser shots. External calibration was performed for molecular mass assignments using a protein calibration standard (ProtCal I, Bruker Daltonics, Leipzig, Germany). A few picograms of each sample were mixed with a protein matrix solution [sinapinic acid in 30:70 (vol/vol) acetonitrile:trifluoroacetic acid 0.1% in water] in a ratio varying between 1:1 and 1:5. The samples were then applied to a stainless-steel sample plate (Bruker Daltonic) and placed into the instrument. A standard method optimized to a mass range of 5–50 kDa was used in the linear and positive mode according to the manufacturer’s instructions.

Cultures of human coronary artery endothelial cells and wound-healing assay

Human coronary artery endothelial cells (HCAECs; PromoCell) were cultured in T-75 flasks in Endothelial Cell Basal Medium MV (Basal Medium; catalog no. C-22220, PromoCell) supplemented with 5% FCS, 0.4% endothelial cell growth supplement, 10 ng/ml epidermal growth factor, 90 µg/ml heparin, 1 µg/ml hydrocortisone (all as components of supplement pack, catalog no. C-39220, PromoCell), 100 U/ml penicillin/streptomycin solution, and 50 ng/ml amphotericin B to yield Complete Medium according to the instructions of the manufacturer. Confluent HCAECs were washed with 15 ml of PBS, trypsinized, and replated in Complete Medium. Experiments were performed with cells at their fifth to eighth passage. The wound-healing assay

was carried out using ibidi™ culture inserts (Ibidi, Planegg, Germany). Approximately 15,000 cells were seeded in each chamber of the insert and cultured for 1 day to reach 90–100% confluency. The cells were then washed with prewarmed HBSS and the insert was removed, after which the cells were incubated in Basal Medium only or in the presence of 1% FCS (PromoCell), apoA-I, or rat chymase-treated apoA-I (25 or 50 µg/ml each) for 10 h. In additional experiments, HCAECs were incubated with untreated or chymase-treated rHDL particles (50 µg/ml) for 10 h and their endothelial healing effect was evaluated using the above described conditions. Images were captured at 30 min intervals using the Cell-IQ system (Chip-Man Technologies, Tampere, Finland) and analyzed by ImageJ software using the “MRI Wound Healing Tool” macro.

RESULTS

Rat cardiac mast cells are activated by 48/80 and by low-flow ischemia in an isolated perfused rat heart model

It has been previously reported that in the perfused Langendorff rat heart system, injection of the noncytotoxic mast cell degranulating 48/80 into the perfusion line results in cardiac mast cell activation (29). Thus, in freshly isolated rat hearts myocardial mast cells were stimulated to degranulate by exposing them to 48/80 (Fig. 1A), after which the hearts were frozen and mast cell degranulation was evaluated by staining the heparin-containing granules with Toluidine blue. **Figure 2** (upper) shows representative myocardial sections containing toluidine-positive mast cells. In Fig. 2, upper left, a typical resting mast cell in the control heart perfused with only buffer is visible. The cell is filled with heparin-positive granules, but due to the presence of several layers of granules in the thick frozen section, individual intracellular granules cannot be distinguished. Two exocytosed granule remnants can be seen in the close vicinity of the resting mast cell (Fig. 2, upper left inset). Such a small degree of spontaneous degranulation is known to occur during preparation and incubation of viable mast cells *in vitro* without any specific stimulation of mast cells (30).

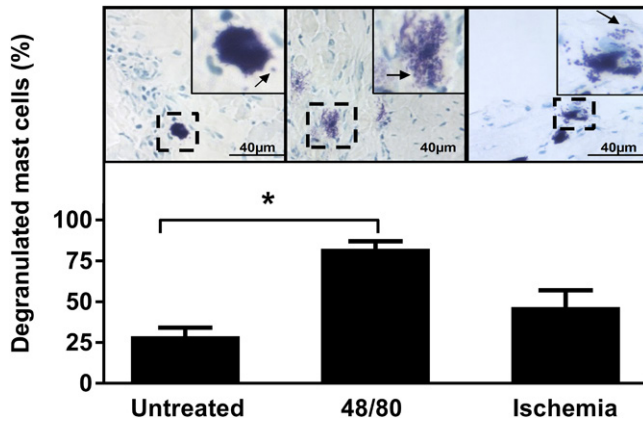


Fig. 2. Cardiac mast cell activation after infusion of 48/80 or induction of low-flow ischemia. The degree of cardiac mast cell activation was evaluated by light microscopy ($\times 40$) from myocardial sections stained with Toluidine blue. Mast cell activation was defined as the presence of extracellular granule remnants extruded into the vicinity of the parent mast cell. Upper: Representative sections of untreated hearts, i.e., perfused with only buffer ($n = 3$ hearts), and hearts in which mast cells had been activated by 48/80 ($n = 3$ hearts) or by induction of myocardial ischemia ($n = 3$ hearts). The arrow in each inset points to one or more extracellularly located granule remnant. Lower: The percentages of degranulated mast cells relative to the total mast cell numbers in each group are shown (the total numbers of mast cells counted in the untreated, 48/80, and ischemia groups were 51, 174, and 214, respectively). Statistical analysis of data from five sections from each heart ($n = 3$ per group) was performed by one-way ANOVA with Dunnett's multiple comparison test. * $P < 0.05$.

Figure 2, upper center shows the effect of 48/80 injection into the perfusion line. Four typical fully ("anaphylactically") degranulated mast cells without any clear cell surface contour are seen (one of them enlarged). We also evaluated mast cell activation under low-flow myocardial ischemia, i.e., a pathophysiological condition which is known to activate mast cells to degranulate in the hypoxic rat heart (17, 20). For this purpose, the flow rate of the perfusion buffer was lowered to 1/10th (0.6 ml/min) (Fig. 1B). As shown in Fig. 2 (upper right), ischemia was found to stimulate mast cell degranulation to a moderate degree. Yet, from the three mast cells visible, one is anaphylactically degranulated (enlarged). We then quantitated the proportion of the degranulated mast cells in various heart preparations (Fig. 2, lower). This analysis demonstrated that 48/80 caused a significant increase in the proportion of degranulated mast cells as compared with the untreated heart serving as a control. Ischemia also induced degranulation, but to a milder degree.

The extent of mast cell activation was also evaluated by measuring histamine levels in the collected heart perfusates (Fig. 3). When compared with the perfusate fractions collected before the treatments (nonactivated, i.e., resting mast cells), in which the histamine concentration was ~ 10 ng/ml, perfusion of the hearts with 48/80 increased the level of histamine by more than 10-fold, indicating that activation of cardiac mast cells with ensuing release of histamine had occurred (Fig. 3A). When cardiac mast cells were activated by ischemia, the histamine levels in the collected

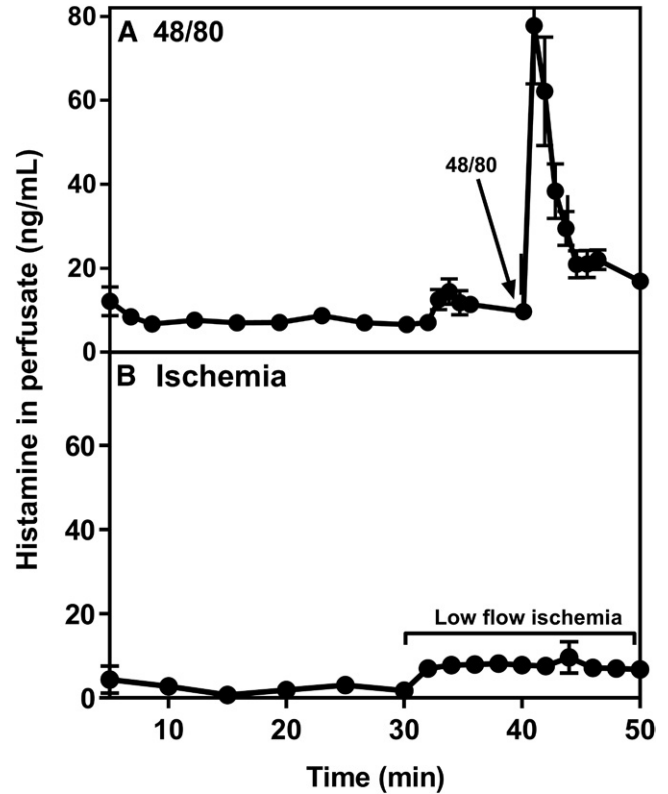


Fig. 3. Histamine levels in coronary effluents. Coronary effluents from hearts treated with 48/80 ($n = 8$) (A) or exposed to low-flow ischemia ($n = 3$) (B) were collected for histamine determination. Coronary effluents were collected following the mast cell-activating protocols described in Fig. 1. Values (mean \pm SEM) are derived from triplicate measurements.

effluent increased by about 4-fold compared with the basal level (Fig. 3B). Thus, the release of histamine under the studied conditions confirmed the morphological observations in that myocardial ischemia in the Langendorff hearts induces mast cell activation, yet to a moderate degree compared with the acute anaphylactic release of histamine induced by 48/80.

Cardiac mast cell activation leads to proteolysis of perfused apoA-I

We next evaluated the proteolytic activity of chymase released from rat cardiac mast cells under the two mast cell activation-inducing protocols by determining the intactness of apoA-I infused into the Langendorff hearts. For this purpose, the collected perfusate samples were analyzed on 4-12% Bis-Tris PAGE gels (Fig. 4A). When apoA-I was perfused into untreated hearts, it eluted as a single band corresponding to the intact apolipoprotein (apparent molecular mass 28 kDa) (Fig. 4A, lane 1). In contrast, the apoA-containing perfusate collected after treatment of the hearts with 48/80 contained two additional polypeptide bands, as reflected by one major band which migrated below the intact apoA-I and another band which was barely visible below the major band (Fig. 4A, lane 2). These two additional polypeptides with apparent molecular masses of 26 and 22 kDa were likely proteolytic products generated when apoA-I was perfused through the 48/80-treated

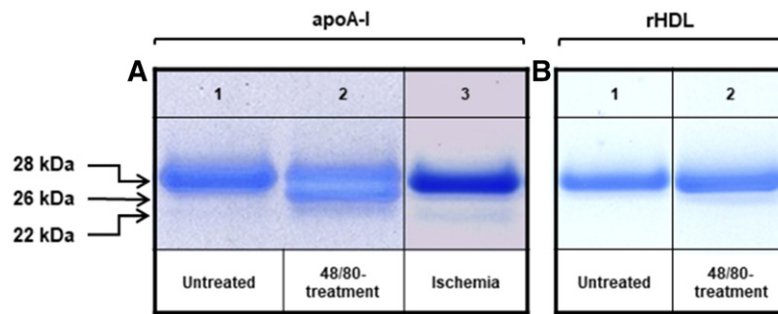


Fig. 4. Proteolysis of apoA-I by activated cardiac mast cells ex vivo. A: A total of 1 mg of ApoA-I was perfused through the Langendorff system following the mast cell-activating protocols shown in Fig. 1, and samples of the perfusate were collected. Shown are representative samples correspond to apoA-I perfused through untreated control hearts ($n = 4$) (lane 1), after treatment with 48/80 ($n = 4$) (lane 2), or after induction of low-flow ischemia ($n = 3$) (lane 3). B: In separate experiments, 1 mg of apoA-I-containing rHDL was perfused through the rat hearts in the Langendorff system, and the intactness of apoA-I was evaluated in control hearts ($n = 1$) (lane 1) and after treatment with 48/80 ($n = 3$) (lane 2). Aliquots (1 μ g of protein) were analyzed by NuPAGE Novex 4-12% Bis-Tris gradient gel, and the protein bands were visualized.

hearts. Induction of ischemia, again, appeared to have a weaker proteolytic effect on apoA-I, as it resulted in the generation of a single degradation product with an apparent molecular mass of 22 kDa, which was detected as a minor band (Fig. 4A, lane 3). The extent of apoA-I degradation achieved in the 48/80-stimulated hearts was 40% and in the ischemic hearts 3%, as evaluated by densitometric scanning of the bands in the electrophoretic gels using the Image Studio™ Lite Software.

Both lipid-free apoA-I and rHDL did flow through the heart at same speed, and the recovery in each case was almost 100%. However, when the apoA-I-containing rHDL preparation was infused into the hearts treated with 48/80 to trigger a robust chymase release from the cardiac mast cells, no signs of apoA-I degradation were detected in the collected perfusates (Fig. 4B).

Identification of apoA-I cleavage sites produced ex vivo in the Langendorff heart confirms that the proteolytic fragments were generated by chymase

The cleavage sites on apoA-I and the molecular masses of the digestion products generated in the Langendorff perfusion system were identified by mass spectrometry (Table 1). This analysis showed that the upper and the lower one of the two generated bands detected by PAGE in the perfusate from the 48/80-treated hearts (Fig. 4A, lane 2) contained polypeptides with molecular masses of 26,458 and 22,395 Da, respectively. These peptides had been produced by cleavage of apoA-I in the C terminus at positions

of aromatic amino acids Phe²²⁹ and Tyr¹⁹², so fully coinciding with the reported cleavage specificity of chymase. Thus, they were identified as proteolytic products generated by activation of cardiac mast cell with ensuing release of chymase. The single proteolytic band detected on the PAGE gel after induction of low-flow ischemia in the rat hearts (Fig. 4A, lane 3) had a molecular mass of 22,395 Da, and, as above, the cleavage site was identified to target residue Tyr¹⁹² of apoA-I. Thus, the detection of identical polypeptide signals by mass spectrometry in the eluents from 48/80-treated hearts and ischemic hearts confirmed that a 22,395 Da proteolytic product derived from apoA-I cleavage at Tyr¹⁹² is generated under both conditions (supplemental Fig. S1).

Weak protein signals corresponding to low-molecular-mass (5–17 kDa) polypeptides were present in the mass spectrum of ischemic samples. The mass-spectrometric in silico data did not, however, fit to any predicted chymase cleavage sites of apoA-I, and thus these polypeptides were confirmed not to be apoA-I fragments originating from chymase-dependent proteolysis. Their appearance in the eluents from the ischemic hearts suggested that they could have resulted from the action of other cardiac proteases, whose activities have been demonstrated to increase in experimental models of ischemia in rat hearts (31), or they could be other proteins or protein fragments released during myocardial ischemia (32). For these reasons, they were considered irrelevant for the purpose of the present work and were not subjected to further analysis.

TABLE 1. Mass spectrometric analysis of apoA-I proteolytic fragments generated in the beating heart after mast cell activation ex vivo

Apparent Molecular Mass	+48/80			Ischemia		
	Molecular Mass	Cleavage Site	Fragment	Molecular Mass	Cleavage Site	Fragment
28	28,080	—	1-243	28,080	—	1-243
26	26,458	Phe ²²⁹	1-229	—	—	—
22	22,395	Tyr ¹⁹²	1-192	22,395	Tyr ¹⁹²	1-192

Aliquots of the perfusates from hearts in which pharmacologic (+48/80) or hypoxic (ischemia) activation of cardiac mast cells was induced (see Fig. 1) were analyzed by mass spectrometry. Intact apoA-I (1-243) and the fragments generated from it are shown.

Proteolytic profiles of apoA-I generated in vitro by chymase present in rat peritoneal mast cell granule remnants and by recombinant human chymase

In order to investigate whether the proteolytic profile of apoA-I generated by the rat chymase would have its counterpart when apoA-I is exposed to human chymase, we studied the time course of proteolysis by both enzymes under conditions of limited proteolysis. For this purpose, we incubated human lipid-free apoA-I (i.e., the standard preparation used in this study) either with rat peritoneal mast cell granule remnants, in which chymase is the sole chymotryptic protease, or with recombinant human chymase. Since we had detected apoA-I fragments in the perfusate samples from 48/80-treated hearts already at 1 min after apoA-I injection, we incubated apoA-I with the chymases at 37°C for short (up to 5 min) and long (up to 120 min) periods of time, and the proteolytic products of apoA-I were analyzed on 4–12% Bis-Tris PAGE gels (Fig. 5). Short treatment of apoA-I with rat chymase (Fig. 5A, right) was found to produce only one major band with apparent molecular mass of 22 kDa, whereas two bands of apparent molecular mass of 26 and 22 kDa were detected after treatment with human chymase (Fig. 5A, left). As judged by the intensities of the protein bands, the initial rate (at 1 min) of apoA-I degradation by the human chymase was faster than that by the rat chymase. However, after 5 min of incubation, the rat enzyme had produced a more significant depletion of the full-length apoA-I with concomitant strong intensification of the detection signal of the 22 kDa band. When incubation with either chymase was prolonged, the band corresponding to intact apoA-I progressively disappeared, and, moreover, it was no more visible at the longest incubation time (120 min) (Fig. 5B). The 22 kDa band predominated at all incubation times with the human chymase, and this polypeptide band was also the only one generated by

the rat chymase. To investigate whether the proteolytic pattern consisting of two polypeptide bands generated by human chymase was due to inactivation of the recombinant enzyme during incubation, we increased the enzyme concentration by 2-fold and prolonged the incubation time for up to 24 h (Fig. 5C). The results demonstrated that increasing the enzyme activity and prolonging the incubation time resulted in a proteolytic profile consisting only of a single 22 kDa band. No additional degradation products with lower molecular mass could be recognized (not shown). Thus, the final proteolytic profiles of apoA-I generated by either rat or human chymase were identical. A higher proteolytic efficiency of the immobilized (granule heparin-bound) rat chymase in comparison with the recombinant human chymase resembles our previous observation showing that the native heparin-bound rat chymase degrades various lipid-free protein substrates more efficiently than isolated and purified rat chymase devoid of heparin (12). This difference probably relates to a more optimal conformation of chymase when it is in its natural environment, i.e., bound to the heparin proteoglycan meshwork of a mast cell granule remnant.

We next verified by Western blotting the identity of the apoA-I cleavage products generated by either chymase. For this purpose, the peptides in the incubation mixtures shown in Fig. 5A, B were electro-transferred onto a nitrocellulose membrane and detected with a monospecific rabbit anti-human apoA-I polyclonal (R261) antibody and with a mouse monoclonal (16-4 Mab) antibody which specifically recognizes a C-terminally truncated 26 kDa apoA-I fragment generated by human chymase (25, 31) (Fig. 6). Consistent with the above results (Fig. 5), the polyclonal antibody recognized 26 and 22 kDa proteolytic apoA-I fragments after incubation of apoA-I with human chymase. This antibody also recognized a single 22 kDa apoA-I fragment

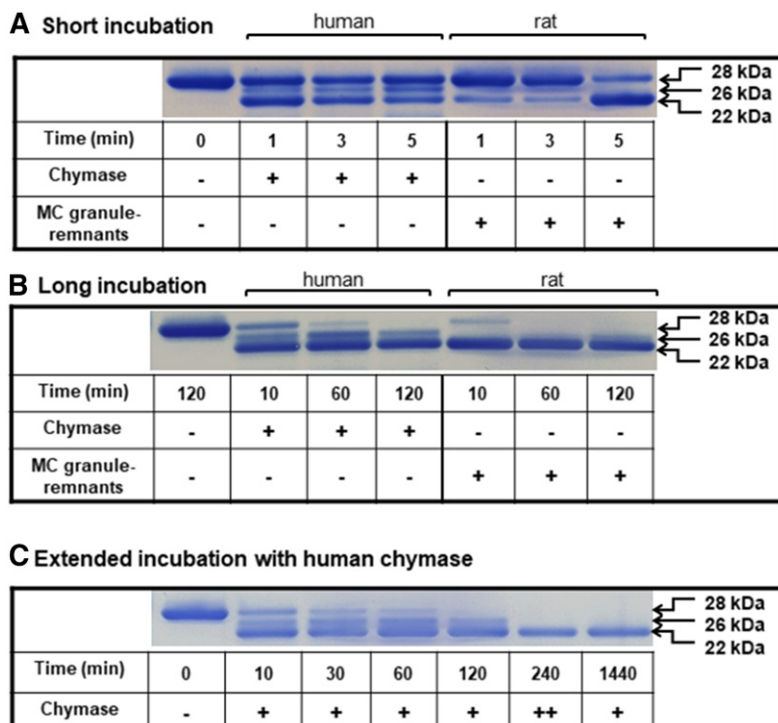


Fig. 5. Proteolysis of apoA-I by human and rat chymase in vitro. ApoA-I (1 mg/ml) was incubated at 37°C in TNE buffer in the presence of recombinant human chymase or rat mast cell chymase-containing granules (40 BTEE units/ml each) for short (up to 5 min; A), long (120 min; B), or extended (C) periods of time. After long incubation with either chymase (B) the band corresponding to intact apoA-I was no more visible. C shows an additional experiment in which the activity of human chymase was increased by adding a second aliquot of the enzyme after 120 min incubation to reach a final activity of 80 BTEE units/ml (denoted as ++), and the incubation was further extended up to 240 min. The last lane shows prolonged incubation of apoA-I with human chymase (40 BTEE units/ml) for up to 1,440 min (24 h). ApoA-I and its proteolytic products in the reaction mixtures were analyzed as described in Fig. 4.

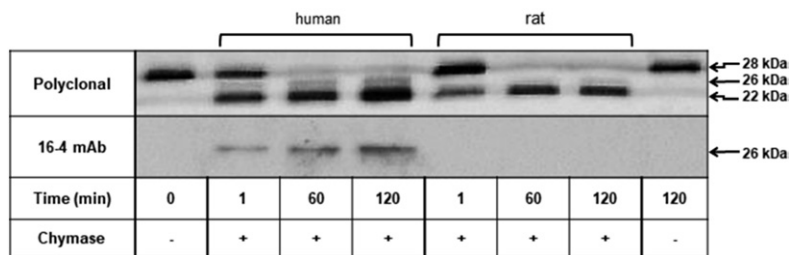


Fig. 6. Identification by site-directed monoclonal antibody of the apoA-I fragment truncated at Phe²²⁵. ApoA-I (1 mg/ml) was incubated in the presence of human or rat chymase for up to 2 h, as described in Fig. 5. Chymase-digested apoA-I fragments were analyzed by 15% SDS-PAGE. Proteins were blotted onto nitrocellulose membrane, after which the membranes were incubated either with rabbit anti-human apoA-I polyclonal antibody (R261) or with 16-4 Mab monoclonal antibody, which specifically reacts with truncated apoA-I at Phe²²⁵. Immune complexes were visualized with HRP-conjugated ECL.

after incubation of apoA-I with rat chymase (Fig. 6, upper blot). In both incubations, the 22 kDa fragment became more prominent as a function of incubation time. Moreover, the 26 kDa protein band present in incubations with the human chymase was also detected with the 16-4 Mab (Fig. 6, lower blot). The reactivity toward the 16-4 Mab confirmed Phe²²⁵ as an additional, yet minor, cleavage site of lipid-free apoA-I by the human chymase (31). As shown below, cleavage at the Phe²²⁵ is not taking place when apoA-I is incubated with the rat chymase in vitro.

Identification of apoA-I cleavage sites produced by rat and human chymase in vitro

The cleavage sites on apoA-I and the molecular masses of the digestion products generated in the setting of short and long incubations by either chymase (Fig. 5) were further identified by mass spectrometry (Table 2). This analysis revealed that the 26,458 and 22,395 Da fragments generated by the exocytosed rat cardiac chymase in the beating heart after 48/80-induced cardiac mast cell activation (Table 1) were also generated in vitro by the human chymase, whereas the rat chymase produced only the 22,395 Da proteolytic fragment in vitro. In addition, the human chymase generated another fragment of 25,964 Da, the cleavage site being at Phe²²⁵. As shown above, with the use of 16-4 Mab, this fragment must have migrated close together with the 26,458 Da fragment as a single band with an apparent molecular mass of 26 kDa in PAGE gels (Fig. 5). This particular polypeptide corresponded to the fragment detected only in incubations with the human chymase, which was specifically recognized by Western blotting with the 16-4 Mab and which has also been detected in human serum (25) (Fig. 6). Overall, the finding that the 22,395 kDa polypeptide generated by cleavage at the site Tyr¹⁹² was the major apoA-I degradation product of both

the rat and human chymase indicated the same proteolytic site specificity of both enzymes regarding the generation of this apoA-I fragment.

Proteolysis of apoA-I by chymase impairs its ability to promote endothelial cell migration

We investigated the ability of apoA-I to stimulate endothelial cell migration and the potential effect of chymase-dependent proteolysis of apoA-I on this function. For this purpose, we incubated HCAECs with intact or chymase-treated apoA-I and examined its effect on the endothelial migration in a wound-healing assay over a period of 10 h (Fig. 7). As serum is known to contain components, including growth factors and HDL that stimulate endothelial cell migration (32), HCAECs were also incubated in FCS as a positive control of the assay. Fig. 7A shows microscopic images of the wound healing area as a function of time when the cells were incubated in Endothelial Cell Basal Medium alone (no addition) or supplemented with FCS, apoA-I, or with a preparation of chymase-treated apoA-I, in which apoA-I had been fully converted into the Tyr¹⁹² fragment (1-192) (Fig. 7B). Compared with the negative control (no addition), addition of apoA-I strongly enhanced the migration of HCAECs. This effect of apoA-I was similar to the observed promigratory effect stimulated by 1% serum. The reduction of the cell-free gap between the endothelial cell fronts promoted by intact apoA-I was time-dependent, and at 10 h the cells formed a dense web, nearly closing the gap area. The reduction in the gap region induced by apoA-I was concentration-dependent. Notably, apoA-I at the higher concentration appeared to exert a stronger effect than that stimulated by 1% serum. As compared with intact apoA-I, the chymase-treated apoA-I displayed a reduced ability to stimulate endothelial cell migration at either concentration. Representative

TABLE 2. Mass spectrometric analysis of apoA-I proteolytic fragments produced by human or rat chymase in vitro

Apparent Molecular Mass	Recombinant Human Chymase			Rat Chymase		
	Molecular Mass	Cleavage site	Fragment	Molecular Mass	Cleavage Site	Fragment
28	28,080	—	1-243	28,080	—	1-243
26	26,458	Phe ²²⁹	1-229	—	—	—
26	25,964	Phe ²²⁵	1-225	—	—	—
22	22,395	Tyr ¹⁹²	1-192	22,395	Tyr ¹⁹²	1-192

Aliquots of the reaction mixtures used for analysis on PAGE gel (see Fig. 5) were analyzed by mass spectrometry. Intact apoA-I (1-243) and apoA-I fragments generated by either human or rat chymase are shown. The analysis reveals that the 26 kDa band generated by human chymase contained two peptides of similar sizes, which comigrated on PAGE gel.

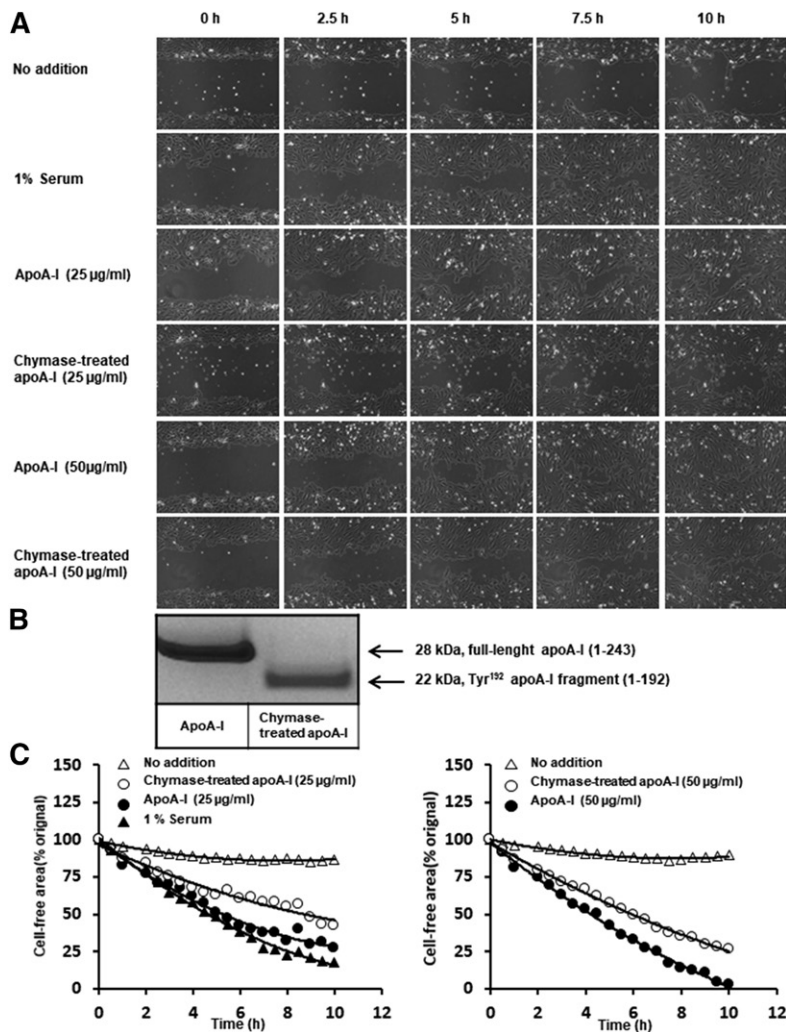


Fig. 7. Effect of chymase-dependent proteolysis of apoA-I on its ability to stimulate endothelial cell migration. Monolayers of HCAECs were plated in the setting of the wound healing assay, as described in Materials and Methods. ApoA-I was proteolyzed with MC granule remnants, and the final apoA-I preparation was chymase-free after sedimenting the granule remnants by centrifugation. HCAECs were incubated with Endothelial Cell Basal Medium (no addition) or in the presence of 1% FCS as a positive control or in the presence of apoA-I or the chymase-treated apoA-I containing the Tyr¹⁹² carboxyl terminal-truncated fragment at the concentrations of 25 and 50 µg/ml each. Cell migration was monitored by using Cell-IQ system for 30-min interval for up to 10 h. A: Micrographs showing the abilities of intact apoA-I and the chymase-treated apoA-I to stimulate cell migration. B: SDS-PAGE gels of the control and proteolyzed apoA-I preparations used in the assay showing, respectively, the intact full-length apoA-I (1-243) and the (Tyr¹⁹²) cleaved apoA-I fragment (1-192). C: The images in A were analyzed by ImageJ software. The cell-free area (percent of initial gap area) is shown as a function of time. The actual migration images of the C right are shown in supplemental Movie S1.

time-lapse photographs showing wound closure in the absence or presence of apoA-I or chymase-treated apoA-I are appended in supplemental Movie S1. These visual observations were confirmed by quantifying the gap areas under the different conditions (Fig. 7C). Overall, these results indicate that truncation of apoA-I at the C terminus by chymase compromised the protective healing effect of apoA-I on human endothelial cells.

Finally, using the above described settings, we evaluated the endothelial healing effect of apoA-I-containing rHDL particles and the effect of chymase on this function (Fig. 8). Whether added in lipid-free or lipidated (rHDL) form, the ability of apoA-I to promote endothelial healing was similar (Fig. 8A, C). Treatment of rHDL with chymase caused only partial (60%) degradation of apoA-I (Fig. 8B), a result which is in line with previous results showing that lipidation of apoA-I renders it partially resistant to proteolysis (33). Yet, treatment of apoA-I and rHDL with chymase impaired their wound-healing abilities to a similar extent.

DISCUSSION

Here, we tested the hypothesis that secretion of mast cell proteases in the ischemic heart could result in inactivation

of the cardioprotective function of lipid-free apoA-I, notably, in promoting endothelial repair. By the use of the Langendorff rat heart perfusion model, we found that in the hypoxic myocardium, the bolus-injected apoA-I becomes exposed to mast cell-derived chymase, which, by cleaving its C-terminal domain, blocks its endothelial healing activity, as examined in an endothelial wound-healing assay *in vitro*. To our knowledge, the present work is the first one to show that chymase-dependent proteolysis of apoA-I occurs in the living heart tissue. The resulting C-terminal trimming of apoA-I compromised its endothelium healing activity, which ultimately could impair its cardioprotective properties (34).

It is well established that cardiac ischemia promotes mast cell degranulation in various mammalian models (17, 20–22) and that ischemia and reperfusion are associated with endothelial injury in the coronary microvasculature (35). Since the myocardial mast cells and the chymase-containing granules released from them reside extravascularly in the myocardial interstitium, the circulating apoA-I, independent of its degree of lipidation, has to cross the endothelial barrier to become exposed to chymase. It is worth noting that, given the high phospholipid binding affinity of apoA-I, a small degree of lipidation of the lipid-free apoA-I infused in aqueous buffer could occur during its

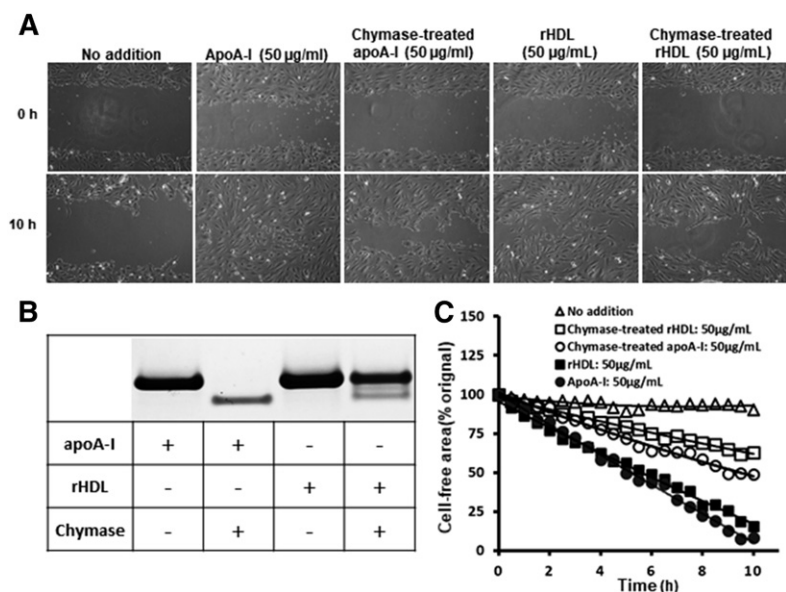


Fig. 8. Effect of chymase-dependent proteolysis of rHDL particles on their ability to stimulate endothelial cell migration. Monolayers of HCAECs were incubated with Endothelial Cell Basal Medium (no addition) or in the presence of apoA-I, chymase-treated apoA-I, rHDL, or chymase-treated rHDL (50 µg/ml each) in the conditions described in Fig. 7. A: SDS-PAGE electrophoresis of the control and proteolyzed apoA-I and rHDL preparations used in the assay showing total proteolytic degradation of apoA-I and partial degradation of rHDL. B: Micrographs showing the abilities of the nontreated and chymase-treated apoA-I and rHDL to stimulate cell migration. C: The images in B were analyzed by ImageJ software. The cell-free area (percent of initial gap area) is shown as a function of time.

rapid passage through the coronary microcirculation. Thus, upon the transient contact with endothelial cells or with the subendothelially located cardiomyocytes, the lipid-free apoA-I could be converted into very poorly lipidated pre β -HDL molecular species, which, like lipid-free apoA-I, should be susceptible to chymase-dependent proteolysis in the subendothelial space (36).

Surprisingly, however, we observed in the Langendorff heart perfusion system that, while 40% of the injected lipid-free apoA-I became C-terminally degraded by chymase, none of the lipidated apoA-I in rHDL (apoA-I:PC:cholesterol:ratio, 1:30:12.5 mol/mol) was degraded. The reason behind the above unexpected finding remains speculative. Basically, two transendothelial routes to the subendothelial space are available for apoA-I: *i*) transcytosis across an endothelial cell and *ii*) paracellular passage via the intercellular space between two endothelial cells. The transcytotic transport mechanisms have been proven to be complex and selective for variously lipidated apoA-I complexes and thereby could potentially retard the transcytotic velocity of certain species of lipidated apoA-I (37). Importantly, however, at sites of mast cell activation, the consequent release of histamine and other vasoactive mast cell-derived compounds causes a marked increase in the microvascular endothelial permeability, resulting from rapid formation of endothelial gaps, particularly in the postcapillary venules (38–40). Such mast cell-dependent gap formation facilitates solvent drag-dependent convective transport of solutes, which includes the transport of globular plasma HDL particles with ($d = 1.063\text{--}1.21\text{ g/ml}$) (41). Actually, in the high-permeability state of a microvascular bed, such a convective mechanism is actually the predominant mechanism for the transendothelial transport of even larger solutes, such as the LDL particles (38, 42).

Interestingly, infusion of a single dose of rHDL (apoA-I:PC-ratio, 1:150 mol/mol) into mice after myocardial ischemia has been found to enhance glucose uptake by cardiomyocytes and to contribute to myocardial salvage after infarction (43). Since direct contact between rHDL and

the cardiomyocytes appeared to be required for such beneficial effect to occur, the rather large discoidal rHDL particles (ranging up to 20 nm in diameter) (44) must have found their way across the microcirculatory coronary endothelium into the interstitial space of the myocardium. Thus, it appears that in the present Langendorff-based experiments, even the histamine-induced leakiness of the myocardial microvascular bed was not sufficient to allow the relatively lipid-poor rHDL particles to become exposed to the subendothelially located chymase and to reenter the coronary circulation for ultimate drainage in the effluente from the heart. Consequently, we are left with the speculation that the rapid passage time, which was about 1 min even during the low-flow of 0.6 ml/min used for the experimentation, and the relative protease-resistance of apoA-I in rHDL particles, jointly contributed to the virtual full resistance of apoA-I in the rHDL particles in the Langendorff heart perfusion system, in which mast cells had been activated. A separate investigation is needed to prove the above hypothesis and to ultimately clarify the mechanistic details of the exit from and the return to the passing perfusion fluid of the lipid-free and rHDL particles and not forgetting the importance of the lymphatic draining operative in vivo.

We also tested the effect of chymase in vitro on the endothelial cell healing ability of rHDL. Importantly, chymase also compromised the ability of such rHDL particles to promote endothelial cell migration and wound repair of human endothelial cells in culture. Indeed, as shown in Fig. 8, only partial degradation of apoA-I in the rHDL particles was sufficient to achieve 50% inhibition of the wound healing, an effect of similar magnitude observed also with fully degraded lipid-free apoA-I. Thus, association of apoA-I with the molar ratios of lipids, such as in rHDL, albeit partly protected apoA-I from chymase-dependent degradation, did not attenuate chymase-dependent reduction in the wound-healing action of rHDL. To resolve this apparent inconsistency, additional detailed kinetic studies are needed.

Proteolytic or genetic deletion of the C-terminal domain (approximately encompassing the amino acid residues

190–243) profoundly affects the functions of apoA-I. Several functional properties of apoA-I are known to depend on the intactness of its C-terminal domain (2), such as its phospholipid binding property and its ability to stimulate ABCA1-dependent cholesterol efflux (45). Moreover, we recently demonstrated that cleavage of the C-terminal region of apoA-I by human mast cell chymase impairs several of its antiinflammatory properties exerted on HCAECs, human neutrophils, and human macrophage foam cells that had been activated by proinflammatory stimuli (33). Our present *in vitro* results provide comparative kinetic data on the chymase-dependent C-terminal truncation of apoA-I by showing that rat chymase promptly (after 1 min incubation) generates only one apoA-I fragment (22,395 Da), which occurs by cleavage of the peptide bond Tyr¹⁹²–His¹⁹³, whereas human chymase generates, in addition, two other C-terminally truncated apoA-I fragments by cleavages at the sites Phe²²⁹–Leu²³⁰ and Phe²²⁵–Lys²²⁶. The cleavage sites found for the human chymase coincide with those previously reported (31). Importantly, when the incubation time was prolonged, the 22,395 Da fragment turned out to be the common proteolytic end-product of both chymases. However, the present experimentation does not provide information on whether there is a precursor-product relationship among the various detected polypeptides. The typical cleavage by either chymase at residue Tyr¹⁹² indicated the high susceptibility of the Tyr¹⁹²–His¹⁹³ peptide bond in the apoA-I polypeptide chain to chymotryptic cleavage. Interestingly, across 31 animal species, the Glu¹⁹¹–Tyr¹⁹² pair is the only completely conserved pair of adjacent residues in apoA-I, and, moreover, this pair is located in a solvent-exposed loop-helix-loop (46), which appears to be critical in facilitating the proteolytic cleavage of apoA-I at Tyr¹⁹², as well as the chlorination of this amino acid residue by myeloperoxidase *in vivo* (47).


Cardiac mast cell activation by treatment with 48/80 or by induction of low-flow ischemia resulted in cardiac mast cell degranulation, which could be confirmed histologically by the presence of extracellular granule remnants and the release of histamine into the perfusion fluid. Induction of degranulation by either treatment did generate C-terminally truncated fragments of apoA-I, yet with different efficiencies. Thus, infusion of apoA-I into the 48/80-treated hearts allowed us to detect the *ex vivo* truncation of apoA-I at the cleavage sites Phe²²⁹ and Tyr¹⁹². Of note, the former cleavage site was absent when apoA-I was incubated with the rat chymase *in vitro*, a finding that could be related to different *ex vivo* and *in vitro* experimental settings, i.e., the rapid passage of infused apoA-I through the heart in contrast to the proteolytic reaction occurring in the test tube, which allowed better exposure of apoA-I to the rat chymase *in vitro*. Low-flow ischemia resulted in the production of only the fragment cleaved at Tyr¹⁹², which further indicated that it is the preferential chymase cleavage site in apoA-I and that this cleavage can occur even upon a moderate degree of mast cell activation, as observed in the hypoxic hearts.

The molecular mechanisms behind the protective endothelial effect of apoA-I and HDL are not fully understood.

Interestingly, however, it was found that HDL can regenerate functional endothelium in damaged New Zealand White rabbit aortas in a SR-B1-dependent and phosphatidylinositol-4,5-bisphosphate 3-kinase/Akt-dependent manner (48). ApoA-I is also a physiological ligand of the F1-ATPase complex *in vivo* (49), and, notably, it was demonstrated that apoA-I improved endothelial cell proliferation via a downstream mechanism initiated by stimulation of F1-ATPase activity (50, 51). Infusion of apoA-I/POPC-containing rHDL can also stimulate the repair of damaged endothelium in mice induced by LPS (52). Thus, enhancement of endothelial repair and improvement of endothelial function appears to be an important function of apoA-I to regenerate a functional endothelium in early atherosclerosis development. This beneficial effect is blunted by HDL nitration and chlorination, which target specific residues of apoA-I susceptible to oxidative damage, suggesting that apoA-I is responsible for this function (53). Moreover, the apoA-I mimetic peptide D4F was recently found to be able to reverse impaired arterial healing in mice *in vivo* and also in bovine aortic endothelial cell cultures (54). However, the specific effect of lipid-free apoA-I to promote endothelial cell migration and endothelial wound healing has not been studied before. Here, we demonstrate that apoA-I in its lipid-free form is able to promote human endothelial cell repair, which indicates that HDL lipids are not required for this function of apoA-I, at least under cell culture conditions. Importantly, our results also demonstrate that the chymase-specific cleavage at Tyr¹⁹² reduced the ability of apoA-I to promote migration of human endothelial cells, so indicating that an intact C-terminal domain in apoA-I is required for the full effect of this property.

The relevance of the above-mentioned finding in relation to the progression of CVDs in humans merits further consideration. Since the number of mast cells and the level of mast cell activation in human atherosclerotic lesions is increased (55), it is feasible that under such pathophysiological conditions, various C-terminally truncated dysfunctional apoA-I fragments are generated. Although the extremely rapid clearance of the proteolytic fragments of apoA-I may constitute a technical limitation for their detection in circulation, with the use of sensitive analytical tools, traces of proteolytic fragments of apoA-I have been detected in plasma from subjects with inflammatory chronic conditions that may have involved activation of mast cells (36). Notably, by aid of the antibody 16-4 Mab generated against the human chymase-digested apoA-I, a chymase-specific fragment truncated at Phe²²⁵ has been detected in normal human serum (25). As increased numbers of mast cells have been reported in human hearts with cardiomyopathy (56), the generation of such fragments could also take place in the ischemic myocardium. Detection of chymase-specific C-terminally truncated fragments of apoA-I in the blood plasma of patients with ischemic heart disease could serve as an additional biomarker of the disease. Development of methods that allow detecting apoA-I-degrading protease activity in living tissues (57) will definitely contribute to a better assessment of the role of proteolyzed apoA-I, e.g., in ischemic heart disease.

The present findings obtained in an ex vivo model of myocardial ischemia resulting in degradation of apoA-I due to release of chymase from hypoxic myocardial mast cells has potential implications for both ischemia- and reperfusion-related injuries of the coronary microvascular system. This suggestion is based on the fact that the loss of cardioprotection actually resulted from apoA-I becoming dysfunctional already during cardiac ischemia. Since myocardial mast cells are long-lived tissue-resident cells and present around myocardial coronary microvessels already in the normally functioning heart, they immediately react to local ischemia and so contribute to the microvascular ischemic injury already in its earliest phase, when the damaging effect on the coronary microcirculation is starting (58). The principal determinants of the microvascular reperfusion injury, again, are considered to be activated circulating neutrophils (59), which, in addition to releasing oxygen free radicals, also release the chymotryptic neutral protease cathepsin G, which, like chymase, degrades apoA-I (33). Thus, a concept emerges, in which activated mast cells initially cause endothelial damage, which, besides triggering loss of endothelial cells (60), also reduces the endothelial wound-healing effect of apoA-I (this study). The initial mast cell-dependent endothelial-damaging mechanisms then generate a preexisting coronary microvascular dysfunction, which are likely to exacerbate the subsequent neutrophil-dependent injury during the reperfusion period.

The strong activation of cardiac mast cells by 48/80 reflects anaphylactic or an anaphylactoid reaction. In several forms of anaphylaxis in man, activation of the heart mast cells contributes to the coronary and also indirectly to the systemic hemodynamic effects by releasing vasoactive mediators, such as histamine and leukotrienes (61). The present work adds one dimension to the mast cell-activation dependent cardiac endothelial dysfunction, namely, release of the neutral protease chymase. Thus, the observation of mast cell activation-dependent acute loss of cardioprotective action of apoA-I during ischemia may provide one explanation to the previous observation demonstrating that, for the preservation of an ischemic myocardial function, HDL needs to be injected into the coronary circulation during the preischemic phase, rather than during the reperfusion phase (18). Moreover, the present results support the notion that, via preventing the cardioprotective actions of apoA-I, the chymase-releasing myocardial mast cells may contribute to damage and dysfunction of both endothelial and myocardial cells in ischemic and anaphylactic conditions. Thus, pharmacological stabilization of mast cells in preischemic myocardium, if practically feasible, would provide a potential target for selective cardioprotective therapy. 

The authors thank Rabah Soliymani for assisting with the mass spectrometry; and Maija Atuegwu, Maria Arraño Kivikko, Mari Jokinen, and Jari Metso for their excellent technical assistance.

REFERENCES

- Asztalos, B. F., M. Tani, and E. J. Schaefer. 2011. Metabolic and functional relevance of HDL subspecies. *Curr. Opin. Lipidol.* **22**: 176–185.
- Lund-Katz, S., and M. C. Phillips. 2010. High density lipoprotein structure-function and role in reverse cholesterol transport. *Subcell. Biochem.* **51**: 183–227.
- Kane, J. P., and M. J. Malloy. 2012. Prebeta-1 HDL and coronary heart disease. *Curr. Opin. Lipidol.* **23**: 367–371.
- Lee-Rueckert, M., F. Blanco-Vaca, P. T. Kovanen, and J. C. Escola-Gil. 2013. The role of the gut in reverse cholesterol transport - Focus on the enterocyte. *Prog. Lipid Res.* **52**: 317–328.
- Miller, N. E., W. L. Olszewski, H. Hattori, I. P. Miller, T. Kujiraoka, T. Oka, T. Iwasaki, and M. N. Nanjee. 2013. Lipoprotein remodeling generates lipid-poor apolipoprotein A-I particles in human interstitial fluid. *Am. J. Physiol. Endocrinol. Metab.* **304**: E321–E328.
- Mineo, C., and P. W. Shaul. 2013. Regulation of signal transduction by HDL. *J. Lipid Res.* **54**: 2315–2324.
- Van Linthout, S., F. Spillmann, G. Graiani, K. Miteva, J. Peng, C. E. Van, M. Meloni, M. Tolle, F. Escher, A. Subasiguller, et al. 2011. Down-regulation of endothelial TLR4 signalling after apo A-I gene transfer contributes to improved survival in an experimental model of lipopolysaccharide-induced inflammation. *J. Mol. Med. (Berl.)* **89**: 151–160.
- Pejler, G., E. Ronnberg, I. Waern, and S. Wernersson. 2010. Mast cell proteases: multifaceted regulators of inflammatory disease. *Blood*. **115**: 4981–4990.
- Lee-Rueckert, M., and P. T. Kovanen. 2015. The mast cell as a pluripotent HDL-modifying effector in atherogenesis: from in vitro to in vivo significance. *Curr. Opin. Lipidol.* **26**: 362–368.
- Urata, H., A. Kinoshita, K. S. Misono, F. M. Bumpus, and A. Husain. 1990. Identification of a highly specific chymase as the major angiotensin II-forming enzyme in the human heart. *J. Biol. Chem.* **265**: 22348–22357.
- Li, J., S. Jubair, and J. S. Janicki. 2015. Estrogen inhibits mast cell chymase release to prevent pressure overload-induced adverse cardiac remodeling. *Hypertension*. **65**: 328–334.
- Lindstedt, L., M. Lee, and P. T. Kovanen. 2001. Chymase bound to heparin is resistant to its natural inhibitors and capable of proteolyzing high density lipoproteins in aortic intimal fluid. *Atherosclerosis*. **155**: 87–97.
- Judström, I., H. Jukkola, J. Metso, M. Jauhiainen, P. T. Kovanen, and M. Lee-Rueckert. 2010. Mast cell-dependent proteolytic modification of HDL particles during anaphylactic shock in the mouse reduces their ability to induce cholesterol efflux from macrophage foam cells ex vivo. *Atherosclerosis*. **208**: 148–154.
- Wang, H., J. da Silva, A. Alencar, G. Zapata-Sudo, M. R. Lin, X. Sun, S. Ahmad, C. M. Ferrario, and L. Groban. 2016. Mast cell inhibition attenuates cardiac remodeling and diastolic dysfunction in middle-aged, ovariectomized Fischer 344 × Brown Norway rats. *J. Cardiovasc. Pharmacol.* **68**: 49–57.
- Shiota, N., J. Rysa, P. T. Kovanen, H. Ruskoaho, J. O. Kokkonen, and K. A. Lindstedt. 2003. A role for cardiac mast cells in the pathogenesis of hypertensive heart disease. *J. Hypertens.* **21**: 1935–1944.
- Oyamada, S., C. Bianchi, S. Takai, L. M. Chu, and F. W. Sellke. 2011. Chymase inhibition reduces infarction and matrix metalloproteinase-9 activation and attenuates inflammation and fibrosis after acute myocardial ischemia/reperfusion. *J. Pharmacol. Exp. Ther.* **339**: 143–151.
- Jaggi, A. S., M. Singh, A. Sharma, D. Singh, and N. Singh. 2007. Cardioprotective effects of mast cell modulators in ischemia-reperfusion-induced injury in rats. *Methods Find. Exp. Clin. Pharmacol.* **29**: 593–600.
- Calabresi, L., G. Rossoni, M. Gomaschi, F. Sisto, F. Berti, and G. Franceschini. 2003. High-density lipoproteins protect isolated rat hearts from ischemia-reperfusion injury by reducing cardiac tumor necrosis factor- α content and enhancing prostaglandin release. *Circ. Res.* **92**: 330–337.
- Rossoni, G., M. Gomaschi, F. Berti, C. R. Sirtori, G. Franceschini, and L. Calabresi. 2004. Synthetic high-density lipoproteins exert cardioprotective effects in myocardial ischemia/reperfusion injury. *J. Pharmacol. Exp. Ther.* **308**: 79–84.
- Gilles, S., S. Zahler, U. Welsch, C. P. Sommerhoff, and B. F. Becker. 2003. Release of TNF- α during myocardial reperfusion depends on oxidative stress and is prevented by mast cell stabilizers. *Cardiovasc. Res.* **60**: 608–616.
- Frangogiannis, N. G., M. L. Lindsey, L. H. Michael, K. A. Youker, R. B. Bressler, L. H. Mendoza, R. N. Spengler, C. W. Smith, and M. L. Entman. 1998. Resident cardiac mast cells degranulate and release preformed TNF- α , initiating the cytokine cascade in experimental canine myocardial ischemia/reperfusion. *Circulation*. **98**: 699–710.

22. Mackins, C. J., S. Kano, N. Seyedi, U. Schafer, A. C. Reid, T. Machida, R. B. Silver, and R. Levi. 2006. Cardiac mast cell-derived renin promotes local angiotensin formation, norepinephrine release, and arrhythmias in ischemia/reperfusion. *J. Clin. Invest.* **116**: 1063–1070.
23. Lindstedt, L., M. Lee, G. R. Castro, J.-C. Fruchart, and P. T. Kovanen. 1996. Chymase in exocytosed rat mast cell granules effectively proteolyzes apolipoprotein A-I-containing lipoproteins, so reducing the cholesterol efflux-inducing ability of serum and aortic intimal fluid. *J. Clin. Invest.* **97**: 2174–2182.
24. Jauhiainen, M., and P. J. Dolphin. 1986. Human plasma lecithin-cholesterol acyltransferase. An elucidation of the catalytic mechanism. *J. Biol. Chem.* **261**: 7032–7043.
25. Usami, Y., K. Matsuda, M. Sugano, N. Ishimine, Y. Kurihara, T. Sumida, K. Yamauchi, and M. Tozuka. 2011. Detection of chymase-digested C-terminally truncated apolipoprotein A-I in normal human serum. *J. Immunol. Methods.* **369**: 51–58.
26. Woodbury, R. G., M. T. Everitt, and H. Neurath. 1981. Mast cell proteases. *Methods Enzymol.* **80**: 588–609.
27. Laine, P., M. Kaartinen, A. Penttilä, P. Panula, T. Paavonen, and P. T. Kovanen. 1999. Association between myocardial infarction and the mast cells in the adventitia of the infarct-related coronary artery. *Circulation.* **99**: 361–369.
28. Shore, P. A., A. Burkhalter, and V. H. Cohn, Jr. 1959. A method for the fluorometric assay of histamine in tissues. *J. Pharmacol. Exp. Ther.* **127**: 182–186.
29. Bispo-da-Silva, L. B., D. O. Sivieri, Jr., C. M. Prado, C. Becari, S. R. Stuckert-Seixas, H. J. Pereira, M. A. Rossi, E. B. Oliveira, and M. C. Salgado. 2010. Cardiac mast cell proteases do not contribute to the regulation of the rat coronary vascular responsiveness to arterial delivered angiotensin I and II. *Vascul. Pharmacol.* **53**: 22–27.
30. Kokkonen, J. O., and P. T. Kovanen. 1985. Low density lipoprotein degradation by rat mast cells: Demonstration of extracellular proteolysis caused by rat mast cell granules. *J. Biol. Chem.* **260**: 14756–14763.
31. Usami, Y., Y. Kobayashi, T. Kameda, A. Miyazaki, K. Matsuda, M. Sugano, K. Kawasaki, Y. Kurihara, T. Kasama, and M. Tozuka. 2012. Identification of sites in apolipoprotein A-I susceptible to chymase and carboxypeptidase A digestion. *Biosci. Rep.* **33**: 49–56.
32. Murugesan, G., G. Sa, and P. L. Fox. 1994. High-density lipoprotein stimulates endothelial cell movement by a mechanism distinct from basic fibroblast growth factor. *Circ. Res.* **74**: 1149–1156.
33. Nguyen, S. D., K. Maaninka, J. Lappalainen, K. Nurmi, J. Metso, K. Oorni, M. Navab, A. M. Fogelman, M. Jauhiainen, M. Lee-Rueckert, et al. 2016. Carboxyl-terminal cleavage of apolipoprotein A-I by human mast cell chymase impairs its anti-inflammatory properties. *Arterioscler. Thromb. Vasc. Biol.* **36**: 274–284.
34. Rye, K. A., and P. J. Barter. 2014. Cardioprotective functions of HDLs. *J. Lipid Res.* **55**: 168–179.
35. Sheridan, F. M., I. M. Dauber, I. F. McMurtry, E. J. Lesnfsky, and L. D. Horwitz. 1991. Role of leukocytes in coronary vascular endothelial injury due to ischemia and reperfusion. *Circ. Res.* **69**: 1566–1574.
36. Lee-Rueckert, M., and P. T. Kovanen. 2011. Extracellular modification of HDL and the evolving concept on the in-vivo proteolytic inactivation of prebeta-HDL as cholesterol acceptors. *Curr. Opin. Lipidol.* **22**: 394–402.
37. Röhrl, C., and H. Stangl. 2013. HDL endocytosis and resecretion. *Biochim. Biophys. Acta.* **1831**: 1626–1633.
38. van Nieuw Amerongen, G. P., R. Draijer, M. A. Vermeer, and V. W. van Hinsbergh. 1998. Transient and prolonged increase in endothelial permeability induced by histamine and thrombin: role of protein kinases, calcium, and RhoA. *Circ. Res.* **83**: 1115–1123.
39. Majno, G., and G. E. Palade. 1961. Studies on inflammation. 1. The effect of histamine and serotonin on vascular permeability: an electron microscopic study. *J. Biophys. Biochem. Cytol.* **11**: 571–605.
40. Ashina, K., Y. Tsubosaka, T. Nakamura, K. Omori, K. Kobayashi, M. Hori, H. Ozaki, and T. Murata. 2015. Histamine induces vascular hyperpermeability by increasing blood flow and endothelial barrier disruption in vivo. *PLoS One.* **10**: e0132367.
41. Kareinen, I., L. Cedó, R. Silvennoinen, P. P. Laurila, M. Jauhiainen, J. Julve, F. Blanco-Vaca, J. C. Escola-Gil, P. T. Kovanen, and M. Lee-Rueckert. 2015. Enhanced vascular permeability facilitates entry of plasma HDL and promotes macrophage-reverse cholesterol transport from skin in mice. *J. Lipid Res.* **56**: 241–253.
42. Rutledge, J. C., F. E. Curry, P. Blanche, and R. M. Krauss. 1995. Solvent drag of LDL across mammalian endothelial barriers with increased permeability. *Am. J. Physiol.* **268**: H1982–H1991.
43. Heywood, S. E., A. L. Richart, D. C. Henstridge, K. Alt, H. Kiriazis, C. Zammit, A. L. Carey, H. L. Kammoun, L. M. Delbridge, M. Reddy, et al. 2017. High-density lipoprotein delivered after myocardial infarction increases cardiac glucose uptake and function in mice. *Sci. Transl. Med.* **9**: eaam6084.
44. Lerch, P. G., V. Fortsch, G. Hodler, and R. Bolli. 1996. Production and characterization of a reconstituted high density lipoprotein for therapeutic applications. *Vox Sang.* **71**: 155–164.
45. Phillips, M. C. 2013. New insights into the determination of HDL structure by apolipoproteins: thematic review series: high density lipoprotein structure, function, and metabolism. *J. Lipid Res.* **54**: 2034–2048.
46. Bashotvyy, D., M. K. Jones, G. M. Anantharamaiah, and J. P. Segrest. 2011. Sequence conservation of apolipoprotein A-I affords novel insights into HDL structure-function. *J. Lipid Res.* **52**: 435–450.
47. Shao, B., M. N. Oda, C. Bergt, X. Fu, P. S. Green, N. Brot, J. F. Oram, and J. W. Heinecke. 2006. Myeloperoxidase impairs ABCA1-dependent cholesterol efflux through methionine oxidation and site-specific tyrosine chlorination of apolipoprotein A-I. *J. Biol. Chem.* **281**: 9001–9004.
48. Wu, B. J., S. Shrestha, K. L. Ong, D. Johns, L. Hou, P. J. Barter, and K. A. Rye. 2015. Cholesteryl ester transfer protein inhibition enhances endothelial repair and improves endothelial function in the rabbit. *Arterioscler. Thromb. Vasc. Biol.* **35**: 628–636.
49. Lyly, A., S. K. Marjavaara, A. Kytälä, K. Uusi-Rauva, K. Lairo, O. Kopra, L. O. Martinez, K. Tanhuanpää, N. Kalkkinen, A. Suomalainen, et al. 2008. Deficiency of the INCL protein Ppt1 results in changes in ectopic F1-ATP synthase and altered cholesterol metabolism. *Hum. Mol. Genet.* **17**: 1406–1417.
50. Radojkovic, C., A. Genoux, V. Pons, G. Combes, H. de Jonge, E. Champagne, C. Rolland, B. Perret, X. Collet, F. Terce, et al. 2009. Stimulation of cell surface F1-ATPase activity by apolipoprotein A-I inhibits endothelial cell apoptosis and promotes proliferation. *Arterioscler. Thromb. Vasc. Biol.* **29**: 1125–1130.
51. Castaing-Berthou, A., N. Malet, C. Radojkovic, C. Cabou, S. Gayral, L. O. Martinez, and M. Laffargue. 2017. PI3Kbeta plays a key role in apolipoprotein A-I-induced endothelial cell proliferation through activation of the Ecto-F1-ATPase/P2Y1 receptors. *Cell. Physiol. Biochem.* **42**: 579–593.
52. Tso, C., G. Martinic, W. H. Fan, C. Rogers, K. A. Rye, and P. J. Barter. 2006. High-density lipoproteins enhance progenitor-mediated endothelium repair in mice. *Arterioscler. Thromb. Vasc. Biol.* **26**: 1144–1149.
53. Pan, B., B. Yu, H. Ren, B. Willard, L. Pan, L. Zu, X. Shen, Y. Ma, X. Li, C. Niu, et al. 2013. High-density lipoprotein nitration and chlorination catalyzed by myeloperoxidase impair its effect of promoting endothelial repair. *Free Radic. Biol. Med.* **60**: 272–281.
54. Rosenbaum, M. A., P. Chaudhuri, B. Abelson, B. N. Cross, and L. M. Graham. 2015. Apolipoprotein A-I mimetic peptide reverses impaired arterial healing after injury by reducing oxidative stress. *Atherosclerosis.* **241**: 709–715.
55. Kaartinen, M., A. Penttilä, and P. T. Kovanen. 1994. Accumulation of activated mast cells in the shoulder region of human coronary atheroma, the prediction site of atheromatous rupture. *Circulation.* **90**: 1669–1678.
56. Janicki, J. S., G. L. Brower, and S. P. Levick. 2015. The emerging prominence of the cardiac mast cell as a potent mediator of adverse myocardial remodeling. *Methods Mol. Biol.* **1220**: 121–139.
57. Maafi, F., B. Li, C. Gebhard, M. R. Brodeur, W. Nachar, L. Villeneuve, F. Lesage, D. Rhainds, E. Rheume, and J. C. Tardif. 2017. Development of a new bioavailable fluorescent probe for quantification of apolipoprotein A-I proteolytic degradation in vitro and in vivo. *Atherosclerosis.* **258**: 8–19.
58. Hollander, M. R., G. A. de Waard, L. S. Konijnenberg, R. M. Meijer-van Putten, C. E. van den Brom, N. Paaui, H. E. De Vries, P. M. van de Ven, J. Aman, G. P. van Nieuw Amerongen, et al. 2016. Correction: Dissecting the effects of ischemia and reperfusion on the coronary microcirculation in a rat model of acute myocardial infarction. *PLoS One.* **11**: e0166809.
59. Niccoli, G., G. Scalone, A. Lerman, and F. Crea. 2016. Coronary microvascular obstruction in acute myocardial infarction. *Eur. Heart J.* **37**: 1024–1033.
60. Mäyränpää, M. I., H. M. Heikkilä, K. A. Lindstedt, A. F. Walls, and P. T. Kovanen. 2006. Desquamation of human coronary artery endothelium by human mast cell proteases: implications for plaque erosion. *Coron. Artery Dis.* **17**: 611–621.
61. Genovese, A., F. W. Rossi, G. Spadaro, M. R. Galdiero, and G. Marone. 2010. Human cardiac mast cells in anaphylaxis. *Chem. Immunol. Allergy.* **95**: 98–109.